

## The modeling of transfer of steering between automated vehicle and human driver using hybrid control framework

Kaustubh, M.; Willemsen, DMC; Mazo Espinosa, Manuel

**DOI**

[10.1109/IVS.2016.7535480](https://doi.org/10.1109/IVS.2016.7535480)

**Publication date**

2016

**Document Version**

Accepted author manuscript

**Published in**

Proceedings of the 2016 IEEE Intelligent Vehicles Symposium

**Citation (APA)**

Kaustubh, M., Willemsen, DMC., & Mazo Espinosa, M. (2016). The modeling of transfer of steering between automated vehicle and human driver using hybrid control framework. In J. Sjöberg, & B. Morris (Eds.), *Proceedings of the 2016 IEEE Intelligent Vehicles Symposium* (pp. 808-814). Article 7535480 IEEE. <https://doi.org/10.1109/IVS.2016.7535480>

**Important note**

To cite this publication, please use the final published version (if applicable). Please check the document version above.

**Copyright**

Other than for strictly personal use, it is not permitted to download, forward or distribute the text or part of it, without the consent of the author(s) and/or copyright holder(s), unless the work is under an open content license such as Creative Commons.

**Takedown policy**

Please contact us and provide details if you believe this document breaches copyrights. We will remove access to the work immediately and investigate your claim.

# The modeling of transfer of steering between automated vehicle and human driver using hybrid control framework

Mani Kaustubh<sup>1</sup>, Dehlia Willemsen<sup>2</sup>, Manuel Mazo Jr.<sup>3</sup>

**Abstract**—Proponents of autonomous driving pursue driverless technologies, whereas others foresee a gradual transition where there will be automated driving systems that share the control of the vehicle with the driver. With such advances it becomes pertinent that the developed automated systems need to be safe. One crucial aspect of safety is to prove that the switching between the human driver and the automated system results in stable system behavior. This paper presents the hybrid control framework used for modeling switching of control authority between manual and automated driving. Also, first results of evaluating stable switching and the inclusion of parameters to address effects of driver comfort and safety are presented. The system developed in this paper consists of an automated driving system that is a combination of a cruise control system and an automated lane keeping system. The manual driving component is modeled as a preview steering controller with a neuromuscular dynamics component. A novel feature of our approach is using the concept of hybrid automata to model the different modes of driving, using the concept of average dwell time to evaluate stability, and using metric interval temporal logic to incorporate verification of different parameters that may affect the switching. We present initial, simulation based results to validate the correctness and usability of the developed framework for future developments.

## I. INTRODUCTION

The continual developments in the field of Advanced Driver Assistance System (ADAS) show a clear trend towards increased automation. These technologies have been found to relieve driver related stress and have resulted in successful accident mitigation leading to increased acceptance. However, the lack of quantitative research on human-automation transfer and reclaiming of control in lateral driving maneuvers necessitates the need for a more human-centered control design. The authors believe although the state-of-art is quite advanced [1] the current approaches to the topic in question are based on a monotonic treatment (i.e. either from the purview of human factors or from systems engineering) and hence, are conservative for a sound analysis of combined human-automation interaction.

The approach outlined in this paper addresses these challenges by developing a conceptual framework for modeling and quantifying interactions between switched systems. Two of the pivotal works in human factors [2] and [4] suggest that a possible solution for flexible and responsive function

allocation is to allocate a task briefly to automation before returning it to human-operator. This argument forms the basis of our research paper. Taking a cue from that, we describe an approach to design and assess the dynamic phenomena underlying the steering interactions that take place during a transfer of control authority between human driver and automated vehicle. The concepts of hybrid automata [3] seemed to fit well to the approaches in the automotive industry of hard switching between the dynamic systems of automated and manual driving. Hence this was taken to analyze the stability by using the concept of average dwell time [16] to evaluate stability of the switching itself. To also take into account intra-personal changes of the driver (driver gain and preview distance) and different driving condition (e.g. longitudinal velocities, maximum allowed lateral deviation and actual take over point) parametric verification using metric interval temporal logic (MITL) [18] was added to the validation scheme that should eventually provide a method to evaluate transition of control designs. The BREACH Matlab toolbox [5] was used to perform the parametric verification of two parameters: Human preview distance and driver gain, which were then varied for different longitudinal velocities, maximum allowed lateral deviation and the time during the lane change when the switch takes place.

Two types of models have been set up. One set to verify the results from the validation scheme in simulation and one to be used in the validation scheme (i.e. the stability analysis and parametric verification). Latter models are linear versions of the simulation models such that the proposed theories could be applied. The Human driver has been modeled as preview controller with a neuromuscular dynamics component for the simulations, whereas for control implementation a linear lead/lag compensator with delay was used [6]. The automated vehicle has been developed using PID control strategy for speed control and PD control strategy for steering control. This research uses a 4 degree-of-freedom (4DOF) ‘two-track’ vehicle model for simulation and after subsequent linearization, the 2DOF vehicle model for stability analysis and parametric verification.

The reason our approach provides a more comprehensive solution to the problem of stable transition of control is because it takes into consideration, three main challenges that arise because of switching between automation and human. Firstly, as presented in a seminal paper [7] (that describes safety implications for automating driving tasks) giving less importance to the impact of human factors leads to erroneous estimation of costs and benefits of automating human-centric tasks. For this reason, this research paper delves equally in

<sup>1</sup>Mani Kaustubh is with the AVL LIST GmbH, Hans-List-Platz 1, 8020 Graz, Austria [mani.kaustubh@outlook.com](mailto:mani.kaustubh@outlook.com)

<sup>2</sup>Dehlia Willemsen is with the Integrated Vehicle Safety Department, TNO, 5700 AT Helmond, The Netherlands [dehlia.willemsen@tno.nl](mailto:dehlia.willemsen@tno.nl)

<sup>3</sup>Manuel Mazo Jr is with the Faculty of Mechanical, Maritime and Materials Engineering, Delft University of Technology [M.Mazo@tudelft.nl](mailto:M.Mazo@tudelft.nl)

human driver modeling as well as in hybrid systems theory. Secondly, our proposed approach is based on already existing advanced driver assistance systems (ADAS) (specifically cruise control and automated lane keeping), thus making it more intuitive for human drivers to adapt and would facilitate acceptance at a later stage. Finally, from [8] in which the authors present an algorithm for synthesis of human-in-loop controllers, it is suggested that human response time becomes significant when controllers are designed to execute transitions between manual and automated modes. This is accounted for in parametric verification of human driving behavior which is described in later sections of this paper.

## II. SYSTEMS MODELING AND CONTROL DESIGN

The basic scenario investigated in this paper needs to be discussed before proceeding to sections on modeling and control. Consider a vehicle following a lane while fully controlled by an automated controller (cruise control system and an automated lane keeping system), referred to as driving in *automated driving mode*. Now, the driver wants to take over steering as there is something on the road ahead (e.g. road damage or ongoing construction) and manually perform a lane change manoeuvre, referred to as driving in *manual driving mode*. It is to be noted that in both cases the speed of the vehicle is always controlled by a cruise controller and also no preceding vehicles are considered to be present in this scenario.

Hybrid automata [9], is a formal model that forms an extension of discrete control graphs, referred to as finite state automata, by incorporating continuous variables. Figure 1 describes an approach to cast the problem of switching between human driver and automated vehicle into the formalism of hybrid automata.

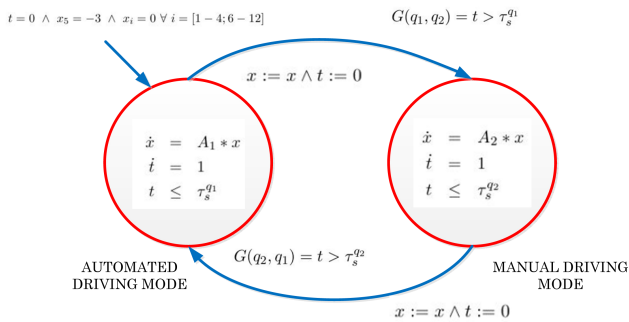


Fig. 1. Graphical representation of hybrid automata describing two states ( $q_1$ ) and ( $q_2$ ), with their invariants, reset maps, guards and the initial state

### Definition 1 (Mode Switching automaton, $\mathcal{H}A$ )

- $Q = \{q_1, q_2\}$ , (Manual Driving mode, Automated Driving mode), are the discrete States.
- $X = [V_y, r, \delta_{st}, \psi, y, \psi, \dot{u}_{ref}, u_{ref}, z, x_1, x_2, m_1, t]^T \forall x \in \mathbb{R}$  and  $t \in \mathbb{R}^+$  are continuous states.
- $I = (0, 0, 0, 0, -3, 0, 0, -3, 0, 0, 0, 0)$  are Initial conditions.
- $f(q_1, x) = A_{1[12 \times 12]}$  and  $f(q_2, x) = A_{2[12 \times 12]}$ , are the flow conditions (refer subsection II-D)

- $Inv = \{q_1, \{t \leq \tau_s^{q_1}, t \in \mathbb{R}^+\}\}, \{q_2, \{t \leq \tau_s^{q_2}, t \in \mathbb{R}^+\}\}$  are the set of invariant conditions, where  $\tau_s^{q_1}$  and  $\tau_s^{q_2}$  are switching times for modes  $q_1$  and  $q_2$  (refer subsection III-C for detailed values)
- $G(q_1, q_2) = \{t \in \mathbb{R}^+ > \tau_s^{q_1}\}$  and  $G(q_2, q_1) = \{t \in \mathbb{R}^+ > \tau_s^{q_2}\}$  where, the guard condition  $G(q_1, q_2)$  denotes the switch from  $q_1 \rightarrow q_2$  and  $G(q_2, q_1)$  denotes the switch from  $q_2 \rightarrow q_1$ .
- $R(q_1, q_2, X) = R(q_2, q_1, X) = \{x\}$ ; which denotes Identity Reset for all states in  $X$  except,  $X_{13} = t := 0$  which is state of the timer and hence is reset to zero.

The continuous states represent the dynamics of the model: The vehicle, the controller and the driver. In the next section these subsystems are introduced.

### A. Vehicle model

The vehicle model used for setting up the hybrid automaton is a two degree of freedom (2DOF) model. This is obtained from linearising a 4DOF non-linear model. [10] suggests that the presence of constant longitudinal velocity and small tire side-slip angles (demonstrating linear tire behaviour) is required to construct a linear vehicle model. Since this research focuses on steering of a vehicle, the longitudinal speed is assumed constant. This can be argued by assuming that driver only takes control of steering while longitudinal vehicle control remains active (i.e. after the driver takes over, the vehicle will still have cruise control active). Also, the tire side slip angles are determined to be similar with low values (lie between  $-0.5^\circ \leq \alpha \leq 0.5^\circ$ ), after applying sinusoidal steering inputs to both the models at constant velocity of 100 km/h for realizing a single lane change of width 3m.

[10] has presented a diagrammatic representation of the 2DOF vehicle model. This paper uses the same model with an ISO axis system. Here,  $V$  is the velocity with  $u$  and  $v$  as longitudinal and lateral decompositions,  $\beta$  is the slip angle (angle of  $V$  with respect to the vehicle center line),  $r$  is the yaw rate,  $\alpha$  is the wheel slip angle,  $\delta$  the steering angle,  $F_y$  the generated lateral tyre force,  $m$  the vehicle mass, and  $I_{zz}$  the moment of inertia around the vehicle top axis. The indexes  $f$  and  $r$  stand for front and rear, respectively.

The tyre force  $F_y$  is assumed to linearly depend on the slip angle  $\alpha$ :  $F_{y_i} = C_{\alpha_i} \alpha_i$ , with  $C_{\alpha_1}$  and  $C_{\alpha_2}$  being front and back tyre stiffness respectively. For a normal car with front steering, this then leads to following linear system representation of the vehicle model:

$$\begin{bmatrix} \dot{v} \\ \dot{r} \end{bmatrix} = \begin{bmatrix} a_{11} & a_{12} \\ a_{21} & a_{22} \end{bmatrix} \begin{bmatrix} v \\ r \end{bmatrix} + \begin{bmatrix} b_{11} \\ b_{21} \end{bmatrix} \delta_f \quad (1)$$

where,

$$\begin{aligned} a_{11} &= -\frac{(C_{\alpha_1} + C_{\alpha_2})}{mu}, & a_{12} &= -\left(u + \frac{aC_{\alpha_1} - bC_{\alpha_2}}{mu}\right) \\ a_{21} &= -\frac{(aC_{\alpha_1} - bC_{\alpha_2})}{uI_{zz}}, & a_{22} &= -\frac{(a^2C_{\alpha_1} + b^2C_{\alpha_2})}{uI_{zz}} \\ b_{11} &= C_{\alpha_1}/m, & b_{21} &= aC_{\alpha_1}/I_{zz} \end{aligned}$$

Since the driver operates the vehicle from the steering wheel, steering dynamics need to be added. The steering wheel is modeled as a second order system with moment of inertia  $J_w$ , stiffness  $K_w$  and damping  $B_w$ . Input to the steering system is a steering torque at the steering wheel  $T_c$ , output is the angle at the front wheels  $\delta_f$ .

### B. The automated steering controller

The automated steering controller realises a steering torque such that a desired trajectory  $u_{ref}$  is followed by the vehicle. The lateral error at a distance  $d_c$  is acted upon by a PD controller with  $C_1$  the proportional gain and  $C_2$  the derivative gain. The derivative action is pre-filtered with filter time constant  $\tau = C_2/10$  (as a rule of thumb):

$$T_c = (C_1 + C_2 \frac{s}{\tau s + 1})e \quad (2)$$

with  $e = (u_{ref} - y - d_c/\psi)$ ,  $y$  the lateral position of the vehicle (integral of lateral vehicle speed  $v$ ) and  $\psi$  the yaw angle (integral of the yaw rate  $r$ ).

### C. The human steering controller

The Human controller presented in this paper is a closed-loop system and its implementation is derived from the Neuromuscular Driver Model [13] and Force-Feedback driver model [14]. The authors present an ‘internal model’ that defines the dynamics resulting from interaction of steering wheel and human arms. The internal model provides a desired torque signal which when applied to steering wheel causes a desired steering angle. Experimental observations (e.g. activation of driver muscles within lane change) done in [13], or model simulations using different driving scenarios in [14] describe the resemblance of the model to real human driving. Figure 2 gives an overview of the system used.

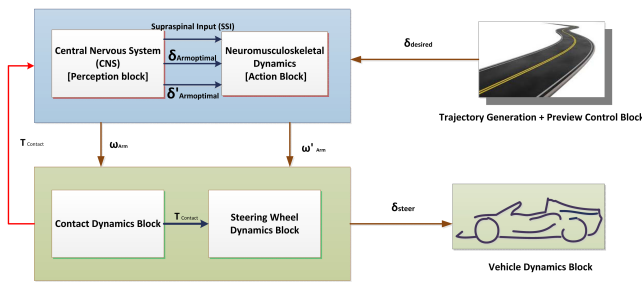


Fig. 2. The Human Driver Model used in this thesis

Figure 3, illustrates driver torque  $T_d$  responses and lateral acceleration responses  $a_y$  for a ‘relaxed’ driver ( $k_p = 1$ ) and a ‘stressed’ driver ( $k_p = 3$ ), where  $k_p$  is human driver gain. As can be observed, application of higher driver gains result in more oscillatory torque responses. This can be attributed to a ‘stressed’ driving behavior at higher gains. Here, the terms relaxed (and stressed) are just qualitative definitions allotted to characterise human driving behavior.

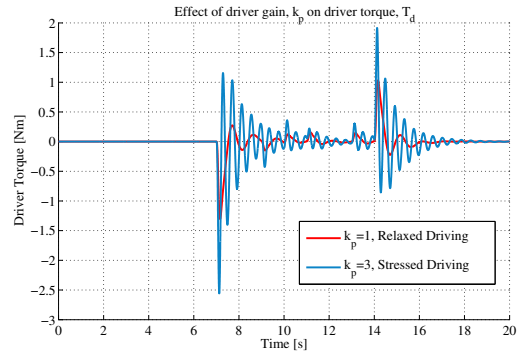


Fig. 3. Observed driver torques for ‘relaxed’ and ‘stressed’ drivers

### D. Formulating the internal dynamics of hybrid automaton

The methodology used to arrive at the equations for an automated controller is to obtain the *state-space* form of the entire plant-controller system. This represents the ‘non-autonomous’ system. Since the stability analysis of hybrid systems in this paper is based on the fact that the states of hybrid automata and their related dynamics are self-contained, there are no ‘exogenous inputs’ to the system that affect its dynamics in any form. By incorporating reference dynamics the non-autonomous state-space system is transformed into its corresponding autonomous form. The controlled system should navigate a lane change, modeled as a second order system  $(s^2 + 2\xi\omega_n s + \omega_n^2)u_{ref} = 0$  reaction to a non-zero initial condition. This leads to following state-space realization of the reference trajectory together with generic plant-controller system:

$$\begin{bmatrix} \dot{X}_i \\ \dot{u}_{ref} \\ \dot{u}_{ref} \end{bmatrix} = \begin{bmatrix} A_i & 0 & B_i \\ 0 & -2\xi\omega_n & -\omega_n^2 \\ 0 & 1 & 0 \end{bmatrix} \begin{bmatrix} X_i \\ u_{ref} \\ u_{ref} \end{bmatrix} \quad (3)$$

where the subscript  $i$  denotes either the automated vehicle (c) or the manual controller vehicle (h).

Then for automated driving following is obtained, with  $X_c = [v, r, \delta_{st}, \delta_{st}, z, y, \psi]^T$  as the system states:

$$A_c = \begin{bmatrix} a_{11} & a_{12} & 0 & b_{11} & 0 & 0 & 0 \\ a_{21} & a_{22} & 0 & b_{12} & 0 & 0 & 0 \\ 0 & 0 & -\frac{B_w}{J_w} & -\frac{K_w}{J_w} & \frac{J_w}{\tau} & -\frac{J_w K}{\tau} & -\frac{J_w K d_c}{\tau} \\ 0 & 0 & 0 & 1 & 0 & 0 & 0 \\ 0 & 0 & 0 & 0 & -\frac{1}{\tau} & \frac{C_2}{\tau} & \frac{C_2 d_c}{\tau} \\ 1 & 0 & 0 & 0 & 0 & 0 & u \\ 0 & 1 & 0 & 0 & 0 & 0 & 0 \end{bmatrix}^T$$

$$B_c = \begin{bmatrix} 0 & 0 & \frac{J_w K}{\tau} & 0 & -\frac{C_2}{\tau} & 0 & 0 \end{bmatrix}^T$$

$$C_c = \begin{bmatrix} 0 & 0 & 0 & 0 & \frac{1}{\tau} & -\frac{K}{\tau} & -\frac{K d_c}{\tau} \end{bmatrix}$$

$$D_c = \begin{bmatrix} \frac{K}{\tau} \end{bmatrix}$$

for manual driving mode the following is obtained, with  $X_h = [v, r, \delta_{st}, \delta_{st}, x_1, x_2, m_1, y, \psi]^T$  as system states:

$$A_h = \begin{bmatrix} a_{11} & a_{12} & 0 & b_{11} & 0 & 0 & 0 & 0 & 0 \\ a_{21} & a_{22} & 0 & b_{12} & 0 & 0 & 0 & 0 & 0 \\ 0 & 0 & -\frac{B_w}{J_w} & -\frac{K_w}{J_w} & J_w \xi_1 & J_w \xi_2 & \frac{J_w K_0}{\tau_d} & -\frac{J_w k_d K_0}{\tau_d} & -\frac{J_w k_d K_0 d_h}{\tau_d} \\ 0 & 0 & 1 & 0 & 0 & 0 & 0 & 0 & 0 \\ 0 & 0 & 0 & 0 & -l_1 & -l_2 & \frac{1}{\tau_d} & -\frac{k_d}{\tau_d} & -\frac{k_d d_h}{\tau_d} \\ 0 & 0 & 0 & 0 & 1 & 0 & 0 & 0 & 0 \\ 0 & 0 & 0 & 0 & 0 & 0 & -\frac{1}{\tau_d} & \frac{C_2 D}{\tau_d} & \frac{C_2 d_h}{\tau_d} \\ 1 & 0 & 0 & 0 & 0 & 0 & 0 & 0 & u \\ 0 & 1 & 0 & 0 & 0 & 0 & 0 & 0 & 0 \end{bmatrix}$$

$$\begin{aligned}
B_h &= \begin{bmatrix} 0 & 0 & \frac{J_w k_d K_0}{\tau_d} & 0 & \frac{k_d}{\tau_d} & 0 & -\frac{C_{2D}}{\tau_d} & 0 & 0 \end{bmatrix}^T, \\
C_h &= \begin{bmatrix} 0 & 0 & 0 & 0 & \xi_1 & \xi_2 & \frac{K_0}{\tau_d} & -\frac{K_0 k_d}{\tau_d} & \frac{K_0 k_d d_h}{\tau_d} \end{bmatrix}, \\
D_h &= \begin{bmatrix} \frac{K_0 k_d}{\tau_d} \end{bmatrix}
\end{aligned}$$

Here dummy variables  $x_1, x_2, m_1, z$  are just mathematical constructs used for obtaining state-space equations for the different modes. Also,  $\delta_{st}$  is input steering angle,  $\tau_L$  is lead constant,  $\tau_I$  is lag constant,  $\tau_d$  and  $\tau_N$  are neuromuscular and action delay constant,  $K = C_1\tau + C_2$  and  $K_0 = -\frac{\tau_L \cdot k_p}{\tau_I}$ . In addition,  $\xi_1 = \tau_L - \frac{(\tau_d + \tau_N)}{2} / \tau_I \frac{(\tau_d + \tau_N)}{2}$ ,  $\xi_2 = k_p / \tau_I \frac{(\tau_d + \tau_N)}{2}$  and  $k_d = C_{1D}\tau_d + C_{2D}$  is where,  $\tau_D = C_{2D}/10$  and  $C_{1D}, C_{2D}$  are PD gains of human controller. Also, it is worth noting that for analyzing the stability of hybrid automata, we proceed by creating equidimensional state-space models for matrices obtained above which will represent ‘continuous’ dynamics in both modes of driving.

### III. SIMULATION AND ANALYSIS

#### A. Experimental scenario

The experimental scenario consists of a *straight* section which is generally the centerline of the current lane, a *curved* section for traversing into the next lane, and a final *straight* section that corresponds to the center line of the next lane. The curved section is modeled as second order system reaction to the initial conditions:  $[\dot{u}_{ref}, u_{ref}] = [0, -3]$ .

#### B. Quantifying the interactions

The parameters presented in this paper fall into two categories: parameters that describe *driver competence* are the Gain bandwidth ( $k_p$ ) and the look-ahead distance of human driver ( $H_{th}$ ). Parameters that describe the ability of a human driver to perceive the changes taking place in surrounding environment, as measured in an interval of space and time, fall in the category *situation awareness*. This paper defines the term Time to Switch or (**TTS**), to quantify driver’s reactive capabilities. The TTS parameter for automated driving mode is  $\tau_s^{q1}$  seconds and the TTS for manual driving mode is  $\tau_s^{q2}$  seconds.

#### C. Stability analysis

Combining the time to switch parameters ( $\tau_s^{q1}, \tau_s^{q2}$ ) and the Time-based Switching theorem developed by Hespanha et. al [16] the average dwell time for the system  $\mathcal{HA}$  to remain stable under switching is given by  $\hat{\tau}_D \geq \hat{\tau}_D^*$  where:

$$\hat{\tau}_D = \frac{\tau_s^{q1} + \tau_s^{q2}}{2} \geq \hat{\tau}_D^* \quad (4)$$

Based on the time based switching theorem, a computational scheme has been set up to determine the value of  $\hat{\tau}_D^*$  involving solving as set of LMIs (whose detailed explanation is beyond the scope of this paper) using the YALMIP [17] Matlab toolbox, that finally resulted in the average dwell time.

$$\frac{\tau_s^{q1} + \tau_s^{q2}}{2} \geq 5.13s \quad (5)$$

**Case I** (When  $\hat{\tau}_D < 5.13$  s): The first scenario we investigate is a lane change of width 3 m and the driver

is supposed to be ill-trained and thus, switches *frequently*. Such an experiment demonstrates the so called *worst-case* scenario. The TTS for each mode will be 1 second i.e.  $\tau_s^{q1} = 1s$  for mode  $q_1$  and  $\tau_s^{q2} = 1s$  for mode  $q_2$ . It has to be pointed out that such a constraint seldom applies to normal highway driving scenarios, but serves as proof of concept for not respecting the Dwell time condition.

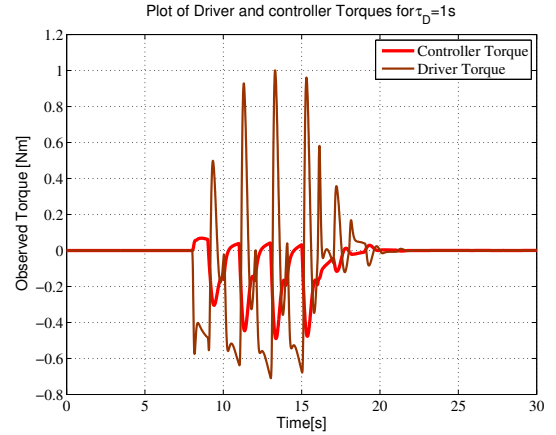


Fig. 4. Driver and controller Torques for  $\hat{\tau}_D^*=1s$

**Case II** (When  $\hat{\tau}_D > 5.13$  s): The system first stays in the  $q_1$  (automated driving mode) for a duration of  $\tau_s^{q1} = 5s$ , then at the instant the vehicle approaches the *curved* section of the lane change maneuver, the mode  $q_2$  (manual driving) is activated for a duration of  $\tau_s^{q2} = 15s$  and finally for the last section, the control is transferred back to the automated vehicle which then steers the vehicle till the end of lane change i.e. the activation time  $\tau_{sk}^{q2} = 10s$ . So, for a simulation time of  $t_{sim} = 30$ , the average dwell time can be calculated by  $\hat{\tau}_D = \frac{\tau_s^{q1} + \tau_s^{q2} + \tau_{sk}^{q1}}{3} = \frac{5+15+10}{3} = 10s$ , which is greater than  $\hat{\tau}_D^* = 5.13s$ .

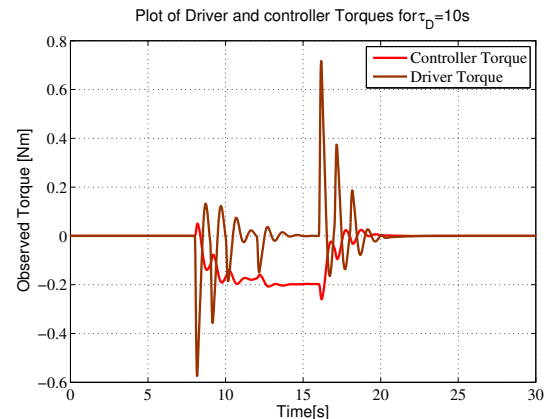


Fig. 5. Driver and controller Torques for  $\hat{\tau}_D^*=10s$

In figure 4 the oscillatory torque responses for driver torques can be explained by the fact that the increase in system energy when a mode switch takes place, is not allowed to dissipate quickly due to inadequate ‘dwell time’

for each mode. Although, the controller torque also shows oscillatory behavior, its values are bounded to between  $-0.6 \leq T_d \leq 0$  Nm. In figure 5 the driver torque values stay bounded between  $-0.6 \leq T_d \leq 0.8$  Nm. The driver torque response successfully decays after perturbations (at the entry and exit of cornering maneuver) thereby confirming the decrease of system energy when ‘dwell time’ for each mode is sufficiently large.

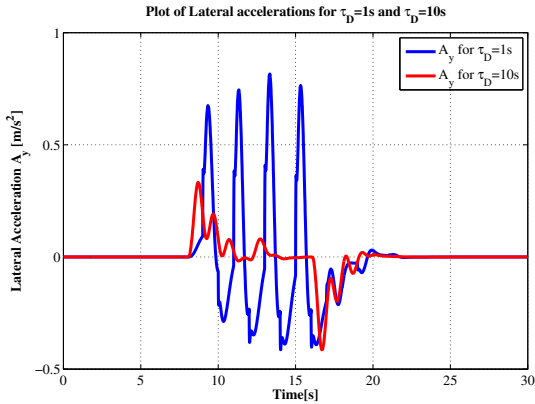


Fig. 6. Lateral Accelerations  $a_y$  for  $\hat{\tau}_D^*=1s$  and for  $\hat{\tau}_D^*=10s$

The lateral accelerations for both the cases are presented in the figure 6. The observed peaks in values of  $A_y$  for  $t_{sim} \approx 7$  s and 17 s, at entry and exit of the *curved* section respectively, result from generation of centripetal forces (tire forces) when cornering on road. However, as can be observed for case II, these oscillations decay quickly to zero when the driver is successful in stabilizing the vehicle on the centerline of road as opposed to case I where the oscillations persist.

#### D. Safety analysis

An experimental approach where parameters attain fixed values, proves conservative for performance analysis on the account that it does not allow one to investigate the complete effects on performance of the system for an exhaustive range of parameters. The calculations in previous section were entirely based on the following parameter values: The look-ahead distance of human driver,  $H_{th} = 15$  m, the preview distance (in automated mode)  $A_{th} = 50$  m, the driver bandwidth  $k_p = 1$ . These are related to the state matrices in equation 3 as follows:  $H_{th} = d_h$   $A_{th} = d_c$ . So in this section, the parameters human preview distance  $H_{th}$  and the driver gain  $k_p$  were varied for different longitudinal velocities  $u$ , maximum allowed lateral deviation  $y_{lat} = y - y_{ref}$  and for different positions during the lane change when the switch takes place, which we refer to by time of switching (ToS).

For the purpose of safety analysis, certain *safety constraints* have been imposed on the switched system to avoid any unsafe lane change maneuvers. These constraints are: yaw rate,  $\dot{\psi} = 0.061$  deg/s, steering wheel rate,  $\dot{\delta} = 0.75$  deg/s and maximum lateral deviation,  $y(t) - y_{ref}(t) \leq 0.3$  m. These values are outcome of closed-loop simulations (Table I) that performed on single mode driving where the human driver navigates a single lane

change of width 3 m at different velocities. A maximum lateral acceleration of  $1.5$  m/s<sup>2</sup> at  $110$  km/h is taken as a reference. In [20] a maximum of  $0.4g$  was registered during normal driving. Considering this as an extreme,  $1.5$  m/s<sup>2</sup> seems a reasonable ‘safety’ bound for normal driving. The values for the safe yaw rate and steering wheel rate then follow from Table I. The lateral deviation constraint is 10% of the lateral displacement. These values serve as nominal values for applying safety constraints during parametric verification using Breach Matlab toolbox.

TABLE I  
CLOSED-LOOP TEST RESULTS: DETERMINING SAFE VALUE RANGES FOR  $\dot{\psi}$  AND  $\dot{\delta}$

Longitudinal Velocity (km/h)	Lateral accelerations (m/s <sup>2</sup> )	Measured Yaw rate ( $\dot{\psi}$ )	Max. absolute Measured SWR ( $\dot{\delta}$ )
80	0.67	0.018	0.375
90	0.71	0.033	0.375
100	0.78	0.0345	0.375
110	0.83	0.035	0.375
80	1.12	0.058	0.75
90	1.25	0.059	0.74
100	1.35	0.061	0.734
110	1.5	0.061	0.72

In terms of a metric interval temporal logic [18] safety constraints are then defined as:

$$\phi = \text{alw} (\dot{\psi} < \alpha_1) \wedge \text{alw} (\dot{\delta} < \alpha_2) \wedge \text{alw} (y - y_{ref} = \alpha_3) \quad (6)$$

where, the constants are then assigned as:  $\alpha_1 = 0.061$ ,  $\alpha_2 = 0.75$ ,  $\alpha_3 = 0.3$  and the keyword *alw* refers to always true condition.

The Figure 7 plots the real and imaginary parts of the poles of the closed loop human-vehicle and automation-vehicle systems for varying  $H_{th}$ . Both the systems had to navigate a single lane change of 3 m at a longitudinal velocity of  $100$  km/h. The plots represent 6 poles for each mode that lie close to origin. From this plot the nominal values for the human preview distance was chosen as  $H_{th} = [13 \ 18]$  m. The intervals for  $A_{th}$  and  $k_p$  were selected in a similar manner resulting in:  $A_{th} = [45 \ 55]$  m and  $k_p = [0.98 \ 1.02]$ .

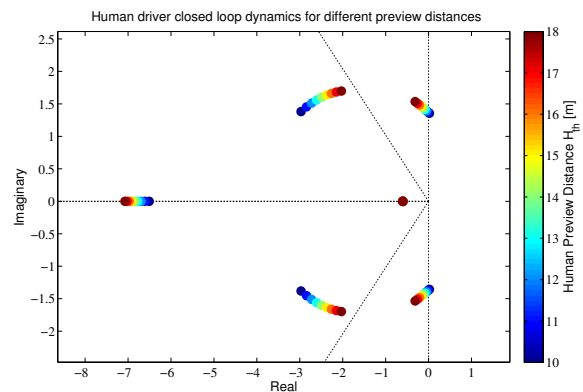


Fig. 7. Selecting the nominal values of parametric intervals for human preview distance  $H_{th}$ .

Now, for performing the said experiments it is important to describe the algorithm that has been referred in this paper for falsification of constraints that in turn leads to obtaining acceptable values of parametric intervals. The *Parameter Synthesis* algorithm described in [19] explains the underlying methodology. The authors base separation of sets into safe, unsafe or uncertain based on an approximation of the reachable set. Developing a parameter synthesis algorithm, this paper utilizes the constraint values on  $\dot{\psi}$ ,  $\dot{\delta}$  and  $y(t) - y_{ref}(t)$  (which are used to define the safe conditions) and runs a falsification algorithm which *terminates* when a falsifying trajectory is encountered and returns the ‘safe’ intervals that respect the mentioned constraints.

a) *Fixed position of switching* : This section describes the parametric verification done to observe the interactions that arise from *switching-to* the manual mode as soon as the vehicle is about to navigate the lane change (vehicle enters the *curved* section). Thus, switching to manual steering mode is only allowed at  $t_{sim} = 0s$ . Steering control is transferred back to automated mode at  $t_{sim} = 20s$ . We use an iterative procedure to observe the inter-related effects of human preview distance, driver gains, and longitudinal velocity when the human driver is in control. An important scenario to analyze is the effect of the velocity  $u$  on driver gains and human preview distances. Figure 8, describes the lateral trajectories as vehicle negotiates a lane change maneuver of width 3m wherein the maximum allowed lateral deviation is 0.3 m. It can be observed that the driver gains have to be *adjusted* with increasing longitudinal velocities if the ‘safety’ constraints have to be respected.

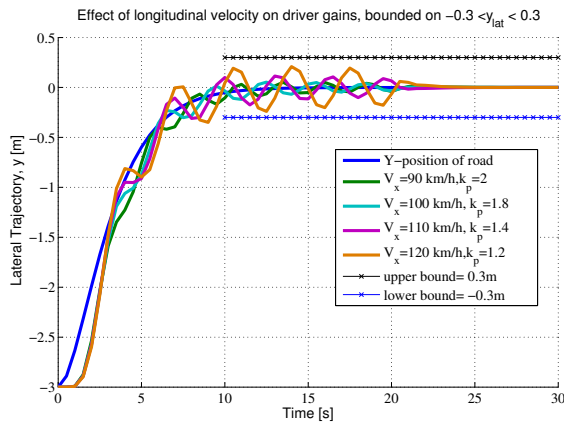


Fig. 8. Verification of driver gain intervals  $k_p$  as observed with variation of the velocity  $u$ . The dotted black and blue lines shows the constraints on maximum allowed lateral deviation  $-0.3 \leq y - y_{ref} \leq 0.3$

b) *Variable position of switching* : In the previous situation, influence of parametric valuations on switching between modes at a fixed position was observed. A next logical step would be to answer the question: What happens when instead of switching after the end of lane change maneuver, one decides to switch at different locations during the maneuver? So, varying time of switching allows the

switching to take place at different positions in a lane change. Although irrespective of when/where one wants to switch modes in a lane change maneuver, the conditions described in equation (5) have to be respected.

Now, to demonstrate the effect of varying instants of mode switching graphically, we assign the driver gain values as  $k_p = 1.2$  for representing a ‘relaxed driver’ and the value  $k_p = 2$  for representing a ‘stressed driver’. For these two types of drivers we then consider two different human preview distance values  $H_{th} = 13$  m and  $H_{th} = 18$  m, describing a driver with smaller and larger look-ahead distances respectively. Figures 9 and 10, illustrate the lane-keeping behavior of a stressed driver, and figures 12 and 11 illustrate those of a relaxed driver. For drivers with same  $k_p$  but different preview distances, larger preview distances lead to better control as the error reduction becomes better with more knowledge of the trajectory. For drivers with different  $k_p$  values, switching later in a lane change ( $ToS \geq 10s$ ) leads to severe oscillations for a stressed driver because of his or her aggressive error control characteristic.

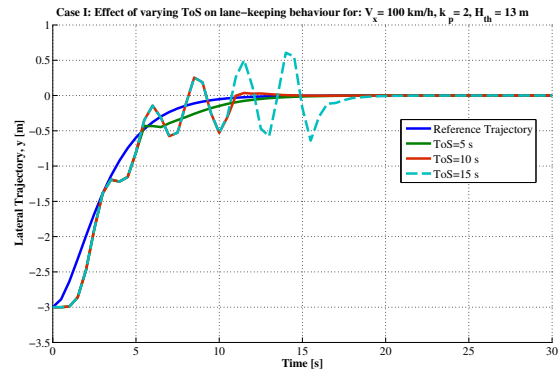


Fig. 9. Effect of varying Time of Switching (ToS) on lane-keeping behaviour for:  $u = 100$  km/h,  $k_p = 2$ ,  $H_{th} = 13$  m

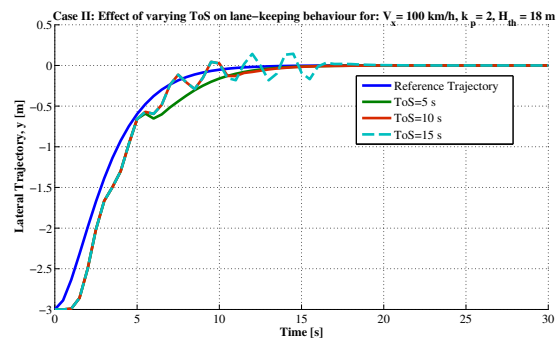


Fig. 10. Effect of varying Time of Switching (ToS) on lane-keeping behaviour for:  $u = 100$  km/h,  $k_p = 2$ ,  $H_{th} = 18$  m

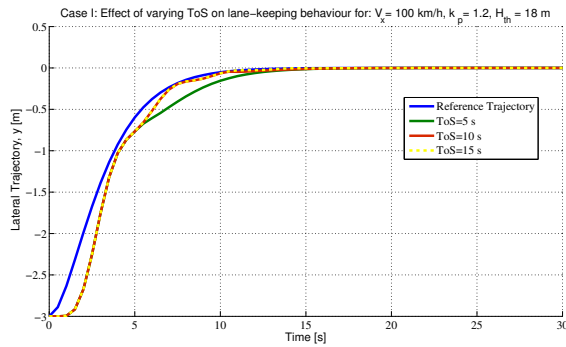


Fig. 11. Effect of varying Time of Switching (ToS) on lane-keeping behaviour for:  $u=100$  km/h,  $k_p=1.2$ ,  $H_{th}=18$  m

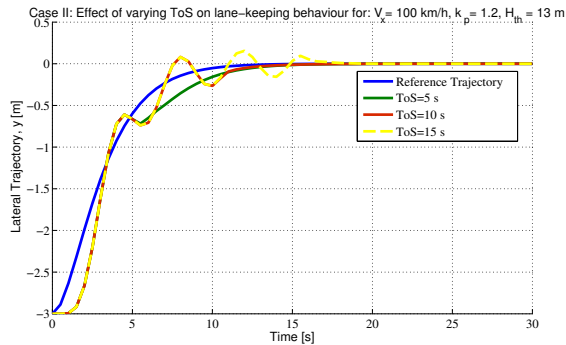


Fig. 12. Effect of varying Time of Switching (ToS) on lane-keeping behaviour for:  $u=100$  km/h,  $k_p=1.2$ ,  $H_{th}=13$  m

#### IV. CONCLUSION AND FUTURE WORK

In this paper, the authors presented the required modeling to come to a ‘primary evaluation scheme’ for analyzing the transition of control between automated and manual driving based on the hybrid systems framework. The results presented in last section, provided a quantitative explanation of the experimental observations made during application of the concepts of switching based on average dwell time and parametric verification of the manual-automated switched system. Apart from further verification of the applied modeling, extending the concept presented in the paper to allow for ‘blending of control’ (instead of an ‘on/off’ approach, i.e. there are continuous periods in which both the modes/controllers are active) could be interesting for future research. Such a scheme would envisage building the model for mixed authority by quantizing the levels of authority of each controller. Also, another interesting extension for future investigations could be to switch between the modes based on applied steering torques. So, the human driver could apply a certain threshold torque so as to not destabilize the vehicle but signal the automation for a take-over of control. Similarly, if the automation observes that the applied driver torques remain bounded within prefixed threshold values for a ‘certain’ duration of time, this would signal it to safely take-over the control of the vehicle. Furthermore, it should be noted that BREACH Matlab toolbox as described by the authors [5] is a simulation-based verification tool. Obtaining

a ‘hard’ guarantee then lies on choosing the grids of separation for refining the parametric intervals ‘sufficiently’ fine. Application of formal methods of verification can help in providing more established ‘formal guarantee’ to the results.

#### REFERENCES

- [1] Seshia, Sanjit A., Dorsa Sadigh, and S. Shankar Sastry, “Formal methods for semi-autonomous driving”, *Proceedings of the 52nd Annual Design Automation Conference*, ACM, 2015.
- [2] Young, Mark S., Neville A. Stanton, and Don Harris, “Driving automation: learning from aviation about design philosophies”, *International Journal of Vehicle Design* 45.3: 323-338, 2007.
- [3] Lygeros, John, Claire Tomlin, and Shankar Sastry. “Hybrid systems: modeling, analysis and control.” *preprint* (1999)
- [4] Parasuraman, Raja, and Victor Riley, “Humans and automation: Use, misuse, disuse, abuse”, *Human Factors: The Journal of the Human Factors and Ergonomics Society* 39.2: 230-253, 1997.
- [5] Donzé, Alexandre. “Breach, a toolbox for verification and parameter synthesis of hybrid systems.” *Computer Aided Verification*. Springer Berlin Heidelberg, 2010.
- [6] Jürgensohn, Thomas. “Control theory models of the driver.” *Modelling driver behaviour in automotive environments*. Springer London, 2007. 277-292.
- [7] Stanton, Neville A., and Philip Marsden, “From fly-by-wire to drive-by-wire: safety implications of automation in vehicles,” *Safety Science* 24.1: 35-49, 1996
- [8] W. Li, D. Sadigh, S. Sastry and S.A. Seshia, “Synthesis of human-in-the-loop control systems”, *Proceedings of the 20th International Conference on Tools and Algorithms for the Construction and Analysis of Systems (TACAS)*, April 2014
- [9] T. Henzinger, P. Kopke, A. Puri, and P. Varaiya, “What’s decidable about hybrid automata”, *In Proceedings of the 27th Annual Symposium on the Theory of Computing*, STOC’95, pages 373-382. ACM Press, 1995.
- [10] Pacejka, Hans, *Tire and vehicle dynamics*. Elsevier, 2005.
- [11] Girard, Antoine, and George J. Pappas, “Verification using simulation”, *Hybrid Systems: Computation and Control*, pages 272-286, Springer Berlin Heidelberg, 2006.
- [12] Lee, John D, “Fifty years of driving safety research”, *Human Factors: The Journal of the Human Factors and Ergonomics Society* 50.3: 521-528, 2008.
- [13] Pick, Andrew J., and David J. Cole, “A mathematical model of driver steering control including neuromuscular dynamics”, *Journal of Dynamic Systems, Measurement, and Control* 130.3: 031004, 2008.
- [14] Katzourakis, D., “Driver steering support interfaces near the vehicle’s handling limits”, TU Delft, Delft University of Technology, 2012.
- [15] Zhai, Guisheng, et al., “Stability analysis of switched systems with stable and unstable subsystems: an average dwell time approach”, *International Journal of Systems Science* 32.8: 1055-1061, 2001.
- [16] Hespanha, Joao P., and A. Stephen Morse, “Stability of switched systems with average dwell-time”, *Decision and Control, Proceedings of the 38th IEEE Conference on*. Vol. 3. IEEE, 1999.
- [17] Lofberg, Johan, “YALMIP: A toolbox for modeling and optimization in MATLAB”, *Computer Aided Control Systems Design, 2004 IEEE International Symposium on*. IEEE, 2004.
- [18] Donzé, A., Maler, O., Bartocci, E., Nickovic, D., Grosu, R., & Smolka, S., “On temporal logic and signal processing”, *Automated Technology for Verification and Analysis*: 92-106, Springer Berlin Heidelberg, 2012.
- [19] Donzé, Alexandre, Gilles Clermont, and Christopher J. Langmead, “Parameter synthesis in nonlinear dynamical systems: Application to systems biology.” *Journal of Computational Biology* 17.3: 325-336, 2010.
- [20] Lechner, D., Perrin, C., “Utilisation réelle des capacités dynamiques des véhicules par les conducteurs [Actual use of vehicle dynamics potential by drivers] (Research Report 165)”, Arcueil, France: Institut National de Recherche sur les Transports et leur Sécurité, 1993.



© 2016 IEEE. Personal use of this material is permitted. Permission from IEEE must be obtained for all other uses, in any current or future media, including reprinting/republishing this material for advertising or promotional purposes, creating new collective works, for resale or redistribution to servers or lists, or reuse of any copyrighted component of this work in other works.